Check for updates

Research Article Vol. 29, No. 2 / 18 January 2021 / Optics Express 674

Optics EXPRESS

InAs/GaAs quantum dot single-section mode-locked lasers on Si (001) with optical self-injection feedback

ZI-HAO WANG,[1,2] WEN-QI WEI,[1,2,3,4] QI FENG,[3] TING WANG,[1,2,3,5] AND JIAN-JUN ZHANG[1,2,3,4,6]

[1] *Beijing National Laboratory for Condensed Matter Physics, Institute of Physics, Chinese Academy of Sciences, Beijing 100190, China*
[2] *Center of Materials Science and Optoelectronic Engineering, University of Chinese Academy of Science, Beijing 100049, China*
[3] *Songshan Lake Materials Laboratory, Dongguan, Guangdong 523808, China*
[4] *State Key Laboratory of Functional Materials for Informatics, Shanghai Institute of Microsystem and Information Technology, Chinese Academy of Sciences, Shanghai 200050, China*
[5] *wangting@iphy.ac.cn*
[6] *jjzhang@iphy.ac.cn*

Abstract: Silicon based InAs quantum dot mode locked lasers (QD-MLLs) are promising to be integrated with silicon photonic integrated circuits (PICs) for optical time division multiplexing (OTDM), wavelength division multiplexing (WDM) and optical clocks. Single section QD-MLL can provide high-frequency optical pulses with low power consumption and low-cost production possibilities. However, the linewidths of the QD-MLLs are larger than quantum well lasers, which generally introduce additional phase noise during optical transmission. Here, we demonstrated a single section MLL monolithically grown on Si (001) substrate with a repetition rate of 23.5 GHz. The 3-dB Radio Frequency (RF) linewidth of the QD-MLL was stabilized at optimized injection current under free running mode. By introducing self-injection feedback locking at a feedback strength of −24dB, the RF linewidth of MLL was significantly narrowed by two orders of magnitude from 900kHz to 8kHz.

© 2021 Optical Society of America under the terms of the OSA Open Access Publishing Agreement

1. Introduction

Semiconductor mode-locked lasers (MLL) are ideal compact solutions to generate high speed optical pulses for applications in optical time division multiplexing (OTDM), wavelength division multiplexing (WDM), and high-speed electro-optic sampling systems [1–3]. Both quantum well (QW) and quantum dot (QD) MLLs have been investigated in the telecom wavelength [4–7]. Compared to QW-MLLs, QD-MLLs benefit from their inhomogeneous gain spectrum and ultrafast carrier dynamics which can help them emit fourier transfer limited ultrafast optical pulses with low timing jitter [1,8]. Besides, InAs/GaAs QD lasers have advantages of low threshold current, high temperature stability and high reflection insensitivity, which make themselves promising for photonic integration applications. In particular, InAs QDs are insensitive to threading dislocations which enable the capability of direct epitaxial growth on Si [9–11]. Over the past decades, direct epitaxially grown InAs/GaAs QD devices on silicon has been extensively explored. A variety of active optoelectronic devices [12–21], including passively mode-locked lasers on silicon [22–24], have been successfully demonstrated to form light sources for silicon photonics. Thus, it is promising to ultimately monolithically integrate the QD-MLL with CMOS compatible silicon photonics integrated circuits (PICs).

Single-section QD-MLLs exhibit advantages of high output power, small footprint, and fabrication simplicity since no saturable absorber section requested, which generally introduce intra-cavity losses. However, the RF linewidth of single-section QD-MLLs is usually realtively

#411551 https://doi.org/10.1364/OE.411551
Journal © 2021 Received 5 Oct 2020; revised 2 Dec 2020; accepted 10 Dec 2020; published 4 Jan 2021

broad in the range of hundreds of kHz, which is not satisfactory for coherent communication applications. Optical feedback as an efficient and practical method has been proven to narrow the linewidth of QD-MLL on the GaAs substrate, both single-section and two-section MLL have been demonstrated to generate low timing jitter, high frequency ultra short optical pulses [23–26]. Recently, coherent feedback has been achieved by adjusting the optical delay line (ODL) in a two-section QD-MLL on silicon [27,28]. In this paper, we proposed to use a simple self-injection feedback setup without ODL on a single-section InAs QD-MLL directly grown on silicon. To the best of our knowledge, it is the first time silicon based single-section InAs QD MLL has been demonstrated by self-injection feedback. By optimizing injection current and feedback strength, the single-cavity QD-MLL shows a repetition rate of 23.5GHz, and the RF linewidth is effectively compressed from 900 kHz to 8 kHz. The paper is organized as follows. We firstly discuss the material growth and fabrication process of single-section QD-MLL on Si (001) substrate. We then present the optimized RF characteristics of the lasers without feedback. Finally, the QD-MLLs are investigated under different self-injection feedback levels. Three mode-locked regimes are observed from RF linewidth evolution spectra. The optimum condition of self-injection feedback is achieved under a coherent feedback level of −24dB.

2. Material growth and device fabrication

The GaAs/Si template and InAs/GaAs QD laser structure were grown in an IV/III-V hybrid molecular beam epitaxy (MBE) system, the schematic diagram of full epitaxial structure is shown in Fig. 1(a). To suppress the APDs, lattice-mismatch induced defects and thermal mismatch between GaAs and Si, specially designed "U"-shape grating patterned Si (001) substrate along [110] direction was fabricated within a CMOS-compatible foundry [9].

By homoepitaxy of Si buffer layer on the "U"-shape patterned Si substrates, the (111)-faceted V-shape Si hollow structures were achieved for subsequent growth of III-V buffer layers and laser structures. For the III-V buffer layer growth, InGaAs/GaAs and InAlAs/GaAs strained layer supperlattices (SLSs) are both deposited as dislocation filter layers (DFLs) to reduce the threading dislocation density (TDD), which is approximately 5×10^6 /cm^2, characterized by electron channeling contrast imaging (ECCI) method. Three periods of AlAs/GaAs superlattices (SLs) are deposited to flatten the surface. A smooth GaAs surface was achieved on Si (001) with a root-mean-square (rms) roughness of 1.2 nm in a 10×10 μm^2 region. The growth details can be also found in our previous work [9].

On the top of 2.2 μm-thick III-V buffer layers, the 4 μm-thick laser structure is then formed. Firstly, 600 nm and 1.4 μm of Si-doped GaAs and $Al_{0.4}Ga_{0.6}As$ were grown as n-contact and n-cladding layers, respectively, followed by a seven layer InAs/GaAs QD active region. Afterward, 1.4 μm and 300 nm C-doped $Al_{0.4}Ga_{0.6}As$ and GaAs were deposited as p-cladding and p-contact layers, respectively. The crystal quality of the III-V layers on Si (001) was characterized by transmission electron microscope (TEM) and room-temperature PL measurements as shown in Fig. 1(b) and (c). The cross-sectional TEM image in Fig. 1(b) indicates that most of the defects are trapped or self-annihilated at the V-shaped GaAs/Si interface region, while the residual defects are filtered by the InGa(Al)As/GaAs SLS structures. Figure 1(c) shows the photoluminescence (PL) comparison of a seven-layer InAs/GaAs QD active region structure grown on GaAs/Si (001) and standard GaAs (001) substrates, respectively. The realtively stronger peak intensity is observed on the GaAs/Si (001) substrate in comparison with that on the GaAs (001) substrate, which is caused by additional reflection from V-shape silicon grating structures [9–11]. The full-width at half-maximum (FWHM) of the PL spectrum on GaAs/Si (001) is measured as 33 meV (GaAs: 35 meV). The inset of Fig. 1(d) shows the 1×1 μm^2 AFM image of the uncapped InAs QDs on GaAs/Si (001) substrate with the dot density of 2.43×10^{10}/cm^2.

The as-grown samples were then processed into ridge lasers with the ridge width varying from 4 μm to 20 μm by using photolithography, dry-etching and metallization. Figure 2(a) shows

Optics EXPRESS

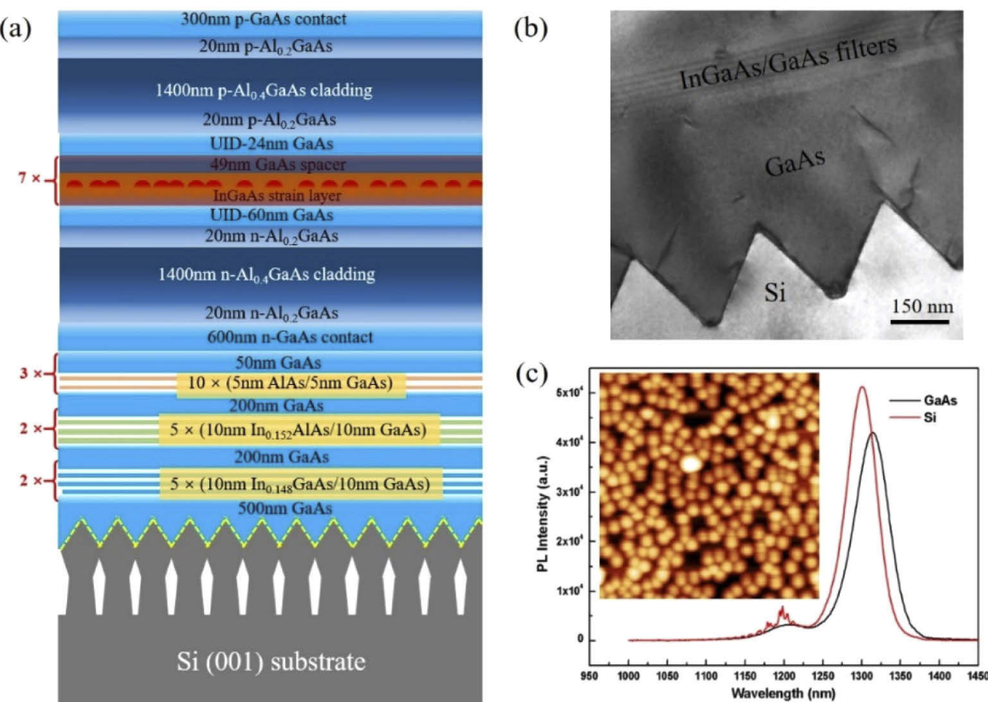

Fig. 1. (a) Schematic diagram of InAs/GaAs QD laser structure grown on Si substrate. (b) Cross-sectional TEM image of the interface between GaAs and Si. (c) Room-temperature PL comparison of a 7-layer InAs/GaAs QD active region grown on GaAs/Si (001) and GaAs (001) substrates, respectively. Inset: 1 × 1 μm^2 AFM image of the uncapped InAs QDs on GaAs/Si (001) substrate.

the schematic diagram of a fabricated InAs/GaAs QD ridge laser on Si (001) substrate with "top-top" contacts. With substrate lapping down to 100 μm, the sample was cleaved into laser bars of different lengths (0.5 mm - 2.5 mm) without any facet coatings. The top right corner of Fig. 2(a) displays the color-enhanced cross-sectional SEM image of a fabricated ridge laser on the Si substrate with a ridge width of 4 μm, which exhibits a clean and mirror-like cavity facet. The continuous wave light-current-voltage (L-I-V) characteristics of monolithically grown single cavity MLL is shown in Fig. 2(b). The laser has a threshold of 120 mA with output power ~9 mW at room temperature (21 °C). The turn on voltage of the diode is ~1V and series resistance is about 14.5 Ω which can be further minimized by improved ohmic contacts. All the RF characteristics hereinafter are measured at 14 °C to ensure the laser has a stable and sufficient output power. The black curve of L-I-V in Fig. 2(b) shows the laser has a threshold and output power of 100mA and 11 mW at 14 °C, respectively.

Optics EXPRESS

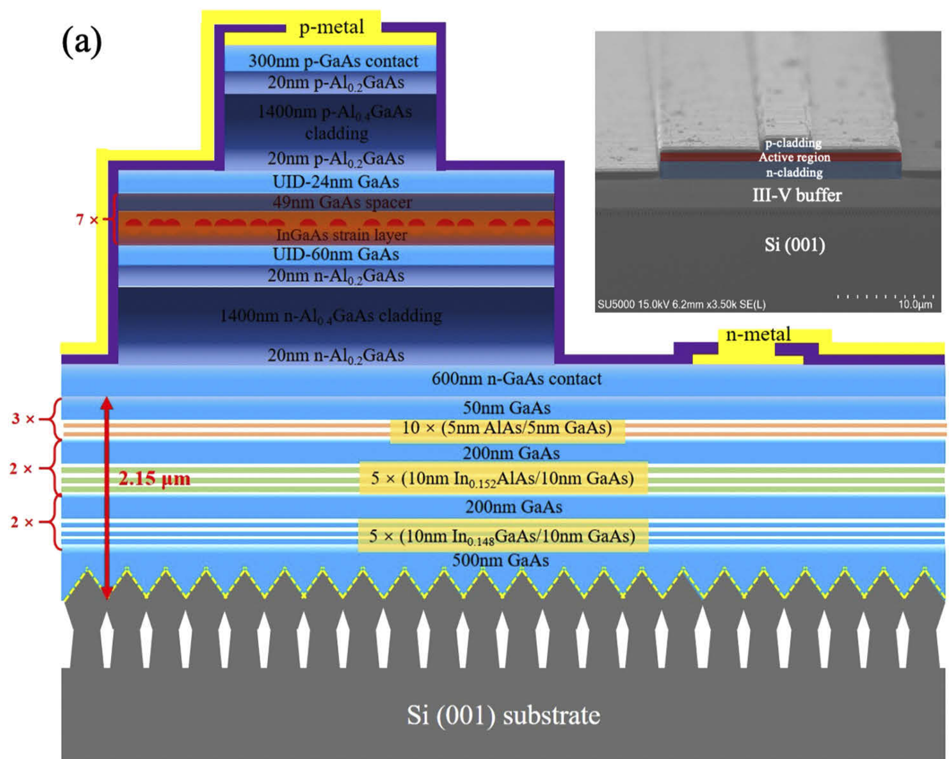

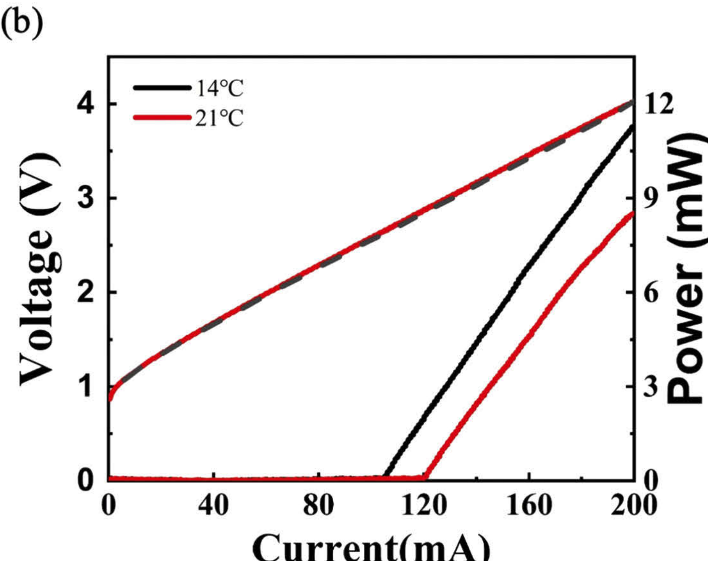

Fig. 2. (a) Schematic diagram of the fabricated InAs/GaAs QD ridge waveguide laser on GaAs/Si (001) substrate. Upper right corner: Color-enhanced SEM image of a fabricated waveguide ridge laser device on Si with the ridge width of 4 μm. (b) L-I-V characteristics of a single section MLL on Si under room temperature (21 °C) and 14 °C

Optics EXPRESS

3. Results and discussion

The RF properties of single-section MLLs are first characterized without external feedback. The schematic of the experimental arrangement is shown in Fig. 3 within the dotted line zone. The laser is mounted on a thermoelectric cooler (TEC) operated at 14 °C for all the measurements. The laser output is collected by a lensed fiber, then splitted into the optical spectrum analyzer (OSA) (Yokogawa AQ6370D) and electrical spectrum analyzer (ESA) (Agilent E4440A) by using a 50/50 fiber coupler. The RF signal is generated by a high speed photodetector (Optilab PD-40M) and amplified with an RF signal amplifier (Optilab MD50) in front of ESA. An isolator is used before splitter to eliminate the reflection from the characterization equipment and a polarization controller (Thorlabs FPC562) is applied to optimize the beam in test setup identical to that of the emitted wave.

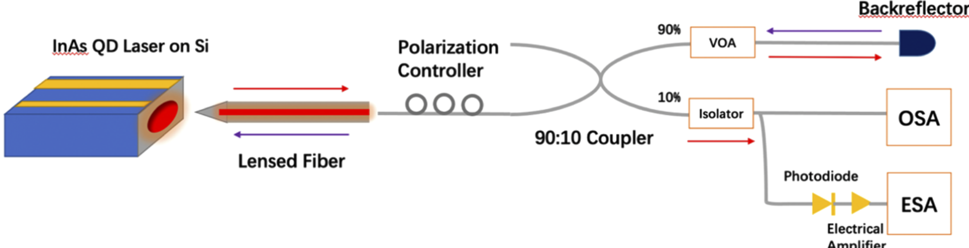

Fig. 3. Schematic of the QD-MLL characterization setup (dotted line zone) and self-injection feedback experimental setup. VOA: variable optical attenuator; OSA: optical spectrum analyzer; ESA: electrical spectrum analyzer

The 2D optical and RF spectra evolutions are simultaneously characterized by injection current spanning from 100 mA to 210 mA as shown in Fig. 4. From Fig. 4(a), the optical spectra show the laser is operated in sole excited state (ES) mode, while the comb spectral bandwith is broadened over 8 nm (Δ−15dB) as current increases to 210 mA. The sole ES lasing is achieved by engineering the free-carrier absorption inside the laser cavity through increasing doping level in the P+ AlGaAs cladding layer. As the result, laser is forced to operate in ES state (higher gain) since the GS gain is not high enough to lase. To note, the reason here chosen a sole ES QD laser on Si is to obtain a stable mode lock operation, as it have been previously proved that dual state QD lasers intend to operate in an unstable mode-lock regime or chaotic mode [29]. From Fig. 4(b), the RF spectra show the single section MLL starts to move into self mode-locking regime at an injection current above 130 mA with a repetition rate of 23.45 GHz which corresponds to the device with 1.8 mm long laser cavity. It is obvious that the RF spectra intend to move into a stable mode-lock regime with narrowed linewidth at a higher injection current above 195 mA. This enhancement is caused by the wide optical bandwidth generated at a higher pumping current level, where more stable coherent comb lines contribute to locking the RF beat frequency signal. It is worth noting that the RF spectrum has unlocked regime between 140 mA to 150 mA, and partially locked regime between 175 mA to 190 mA, respectively. It is due to the fact that the relative phase angles between each fabry-perot modes are not able to fully compensate for the GaAs intracavity dispersion and carrier induced refractive index change. This effect has been simulated and discussed in [29], where a ground state InAs single-section MLL has several partial mode-locking zones under current injection from 2 $\times I_{th}$ to 6.5 $\times I_{th}$.

The single section MLL self-injection characteristics are then investigated with an external feedback setup depicted in Fig. 3. In addition to previous non-feedback experimental arrangement, a 90/10 optical fiber splitter is introduced after the polarization controller and connected with a high reflection (>95%) fiber mirror (Thorlabs P5-1060PMR-P01-1) as a back reflector. The optical feedback intensity is controlled by changing the voltage of a variable optical attenuator

Optics EXPRESS

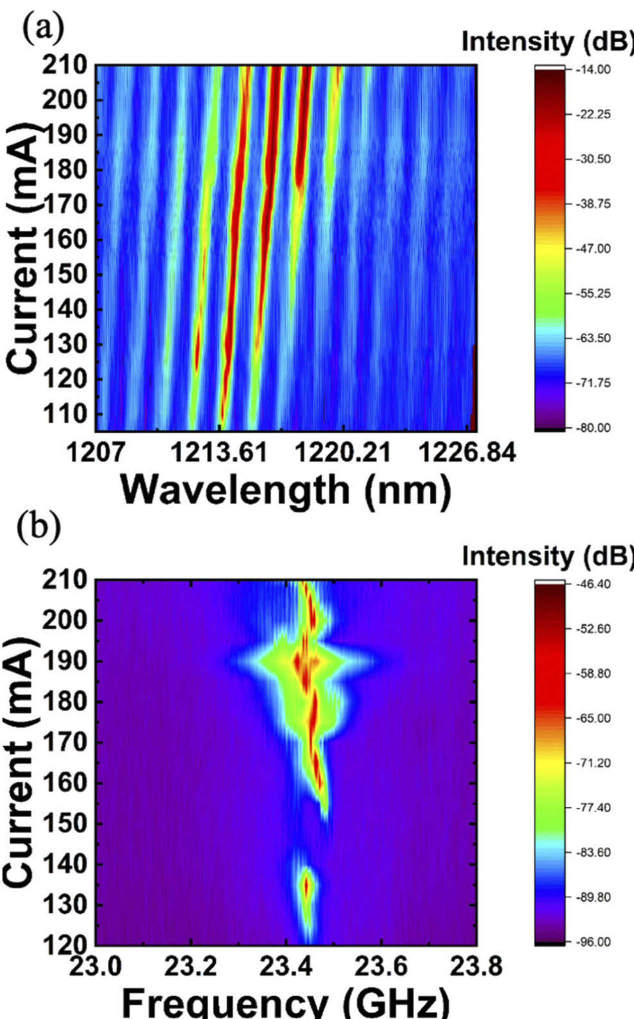

Fig. 4. (a) Optical and (b) RF spectra evolutions with injection current from 100 mA to 210 mA.

(Thorlabs V1000PA) placed between 90% splitter output port and back reflector. The feedback strength is defined as the optical power ratio between laser output power and the power reflected back into laser facet after one round trip through the external cavity. The insertion losses produced in the lens fiber, VOA, polarizer controller and each connector are carefully calibrated.

By adding self-injection feedback, the RF linewidth of single section MLL is optimized firstly by applying injection current from threshold to 195 mA with minimum reflection from VOA. The MLL performs a strong and stable RF beat signal with current injection over 195 mA which aligns with the results of the free running condition. This pre-optimization process seems essential to achieve the coherent feedback without ODL. In the following feedback strength dependent experiments, the MLL is biased at 195 mA. Figure 5(a) shows the RF linewidth evolution of MLL under feedback strength from −10 dB to −45 dB by adjusting the voltage of VOA from 1.5 V to 4 V. It is obvious that there are three different regimes as the feedback strength decreased. This phenomenon has also been observed in the self-injection feedback on quantum dash MLL [30]. The MLL shows coherence collapse under feedback strength higher

Optics EXPRESS

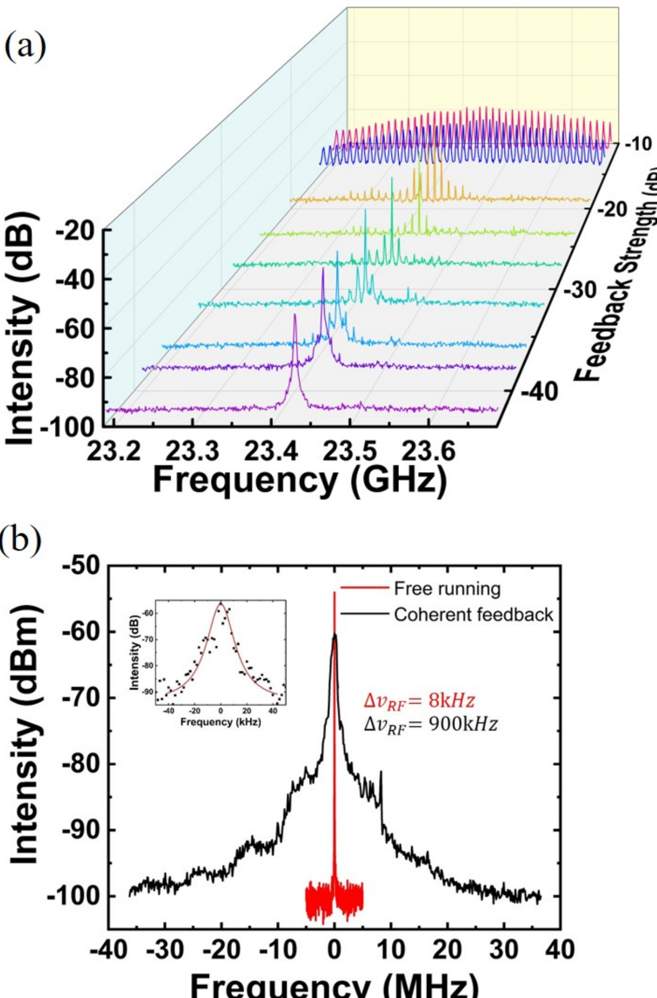

Fig. 5. (a) Evolution of RF linewidth with feedback strength varied from −12 dB to −45 dB under 195 mA injection current. (b) RF spectrum at 23.4 GHz with optimized coherent feedback (−24 dB feedback strength) (red curve) and free running laser (black curve), both are measured under 195 mA injection current.

Optics EXPRESS

than −15 dB. The RF linewidth is broadened by several comb frequency peaks with identical spacing of ~11 MHz which corresponds to a 9 meters long external fiber cavity. This indicates the intracavity longitudinal modes are becoming out of phase at a feedback level higher than −15 dB. As a result, the RF linewidth of the laser is significantly broaden, while moving into the unlocked coherence collapse regime. As the feedback strength gets weaker, the linewidth of the RF beat signal starts to narrow down rapidly, while the MLL shifts into the full self-injection locking regime. The narrowest beat signal is observed at a feedback strength of −24 dB. The central line in the RF spectrum has a signal to noise ratio over 50 dB; the sidebands are suppressed by at least 30 dB. With the feedback strength lower than −38 dB, the RF linewidth begins to broaden. The linewidth of this regime is similar to the QD-MLL operated under optimum bias current in free running case as discussed above since the feedback strength is too week to influence the active laser cavity.

Figure 5(b) shows the high resolution RF spectra that compared the RF linewidth between free running single-section MLL and the one under optimized self-injection locking condition. It shows the 3 dB bandwidth of RF linewidth is ~900 kHz in free running condition and narrows down to ~8 kHz with an optimum feedback strength of −24 dB. The linewidth of RF beating signals are related to timing jitter properties [31]. The pulse to pulse RMS timing jitter of high repetition rate MLL can be calculated as:

$$\sigma_{ptp} = \frac{1}{\nu_0}\sqrt{\frac{\Delta\upsilon}{2\pi\nu_0}} \tag{1}$$

where $\Delta\upsilon$ is the 3 dB RF linewidth and υ_0 is the repetition rate of MLL. According to Eq. (1), the pulse to pulse timing jitter of MLL is reduced by a factor of 10.8 to 10 fs/cycle under the full self-injection locking regime.

4. Conclusion

In this work, we have successfully demonstrated a narrow RF linewidth single-section QD-MLL on Si substrate by optical self-injection locking. The Si-based single-section QD-MLL is investigated under free running conditions with a stable mode-locking RF beat signal of 23.45 GHz at injection current higher than 195 mA. With the self-injection feedback, three major feedback regimes are observed under different feedback levels. The RF linewidth is significantly reduced by two order of magnitude to 8 kHz under the feedback strength of −24 dB. Potentially, single-section Si-based InAs QD-MLL can be monolithically integrated with a silicon photonic feedback loop to achieve coherent feedback conditions on chip. Overall, the realization of self-injection locking by using Si-based single-section InAs QD-MLL is a promising solution to integrate a low timing jitter, low phase noise and high frequency mode-locked optical sources with silicon photonic integrated devices.

Funding. Guangdong Provincial Applied Science and Technology Research and Development Program (2019B121204003); National Natural Science Foundation of China (11804382, 61635011, 61804177, 61975230); National Key Research and Development Program of China (2018YFB2200104); Beijing Municipal Science and Technology Commission (Z191100004819010); Chinese Academy of Sciences Key Project (QYZDB-SSW-JSC009); Youth Innovation Promotion Association of the Chinese Academy of Sciences (2018011).

Acknowledgement. The authors would like to thank Miss Jingjing Guo, Mr. Mingchen Guo and Mr. Kaiyue Hou for their constructive contributions in material growth and device fabrications.

Disclosures. The authors declare no conflicts of interest.

References

1. E. U. Rafailov, M. A. Cataluna, and W. Sibbett, "Mode-locked quantum-dot lasers," Nat. Photonics **1**(7), 395–401 (2007).
2. A. A. Aboketaf, A. W. Elshaari, and S. F. Preble, "Optical time division multiplexer on silicon chip," Opt. Express **18**(13), 13529–13535 (2010).

3. G. Kurczveil, D. Liang, M. Fiorentino, and R. G. Beausoleil, "Robust hybrid quantum dot laser for integrated silicon photonics," Opt. Express **24**(14), 16167–16174 (2016).
4. Z. G. Lu, J. R. Liu, S. Raymond, P. J. Poole, P. J. Barrios, and D. Poitras, "312-fs pulse generation from a passive C-band InAs/InP quantum dot mode-locked laser," Opt. Express **16**(14), 10835–10840 (2008).
5. X. Huang, A. Stintz, H. Li, L. F. Lester, J. Cheng, and K. J. Malloy, "Passive mode-locking in 1.3 μm two-section InAs quantum dot lasers," Appl. Phys. Lett. **78**(19), 2825–2827 (2001).
6. S. Sanders, L. Eng, J. Paslaski, and A. Yariv, "108 GHz passive mode locking of a multiple quantum well semiconductor laser with an intracavity absorber," Appl. Phys. Lett. **56**(4), 310–311 (1990).
7. Z. Wang, M. L. Fanto, J. A. Steidle, A. A. Aboketaf, N. A. Rummage, P. M. Thomas, C.-S. Lee, W. Guo, L. F. Lester, and S. F. Preble, "Passively mode-locked InAs quantum dot lasers on a silicon substrate by Pd-GaAs wafer bonding," Appl. Phys. Lett. **110**(14), 141110 (2017).
8. C. Y. Lin, F. Grillot, Y. Li, R. Raghunathan, and L. F. Lester, "Characterization of timing jitter in a 5 GHz quantum dot passively mode-locked laser," Opt. Express **18**(21), 21932–21937 (2010).
9. W. Q. Wei, J. H. Wang, B. Zhang, J. Y. Zhang, H. L. Wang, Q. Feng, H. X. Xu, T. Wang, and J. J. Zhang, "InAs QDs on (111)-faceted Si (001) hollow substrates with strong emission at 1300 nm and 1550 nm," Appl. Phys. Lett. **113**(5), 053107 (2018).
10. W. Q. Wei, J. H. Wang, J. Y. Zhang, Q. Feng, Z. Wang, H. X. Xu, T. Wang, and J. J. Zhang, "A CMOS Compatible Si Template with (111) Facets for Direct Epitaxial Growth of III–V Materials," Chin. Phys. Lett. **37**(2), 024203 (2020).
11. W. Q. Wei, J. H. Wang, Y. Gong, J. A. Shi, L. Gu, H. X. Xu, T. Wang, and J. J. Zhang, "C/L-band emission of InAs QDs monolithically grown on Ge substrate," Opt. Mater. Express **7**(8), 2955–2961 (2017).
12. T. Wang, H. Liu, A. Lee, F. Pozzi, and A. Seeds, "1.3-μm InAs/GaAs quantum-dot lasers monolithically grown on Si substrates," Opt. Express **19**(12), 11381–11386 (2011).
13. B. Zhang, W. Q. Wei, J. H. Wang, J. Y. Zhang, H. Cong, Q. Feng, T. Wang, and J. J. Zhang, "nm InAs quantum-dot microdisk lasers on SOI by hybrid epitaxy," Opt. Express **27**(14), 19348 (2019).
14. B. Zhang, W. Q. Wei, J. H. Wang, H. L. Wang, Z. Zhao, L. Liu, H. Cong, Q. Feng, H. Liu, T. Wang, and J. J. Zhang, "O-band InAs/GaAs quantum-dot microcavity laser on Si (001) hollow substrate by in-situ hybrid epitaxy," AIP Adv. **9**(1), 015331 (2019).
15. Q. Feng, W. Q. Wei, B. Zhang, H. L. Wang, J. H. Wang, H. Cong, T. Wang, and J. J. Zhang, "O-Band and C/L-Band III-V Quantum Dot Lasers Monolithically Grown on Ge and Si Substrate," Appl. Sci. **9**(3), 385 (2019).
16. W. Q. Wei, J. Y. Zhang, J. H. Wang, H. Cong, J. J. Guo, Z. H. Wang, H. X. Xu, T. Wang, and J. J. Zhang, "Phosphorus-free 1.5 μm InAs quantum-dot microdisk lasers on metamorphic InGaAs/SOI platform," Opt. Lett. **45**(7), 2042 (2020).
17. W. Q. Wei, Q. Feng, J. J. Guo, M. C. Guo, J. H. Wang, Z. H. Wang, T. Wang, and J. J. Zhang, "InAs/GaAs quantum dot narrow ridge lasers epitaxially grown on SOI substrates for silicon photonic integration," Opt. Express **28**(18), 26555 (2020).
18. S. Chen, W. Li, J. Wu, Q. Jiang, M. Tang, S. Shutts, S. N. Elliott, A. Sobiesierski, A. J. Seeds, and I. Ross, "Electrically pumped continuous-wave III–V quantum dot lasers on silicon," Nat. Photonics **10**(5), 307–311 (2016).
19. A. Y. Liu, C. Zhang, J. Norman, A. Snyder, D. Lubyshev, J. M. Fastenau, A. W. K. Liu, A. C. Gossard, and J. E. Bowers, "High performance continuous wave 1.3 μm quantum dot lasers on silicon," Appl. Phys. Lett. **104**(4), 041104 (2014).
20. Y. Wan, J. Norman, Q. Li, M. J. Kennedy, D. Liang, C. Zhang, D. Huang, Z. Zhang, A. Y. Liu, and A. Torres, "1.3 μm submilliamp threshold quantum dot micro-lasers on Si," Optica **4**(8), 940–944 (2017).
21. W. Q. Wei, Q. Feng, Z. H. Wang, T. Wang, and J. J. Zhang, "Perspective: optically-pumped III–V quantum dot microcavity lasers via CMOS compatible patterned Si (001) substrates," J. Semicond. **40**(10), 101303 (2019).
22. S. Liu, X. Wu, D. Jung, J. C. Norman, M. J. Kennedy, H. K. Tsang, A. C. Gossard, and J. E. Bowers, "High-channel-count 20 GHz passively mode-locked quantum dot laser directly grown on Si with 4.1 Tbit/s transmission capacity," Optica **6**(2), 128–134 (2019).
23. C. Y. Lin, F. Grillot, Y. Li, R. Raghunathan, and L. F. Lester, "Microwave characterization and stabilization of timing jitter in a quantum-dot passively mode-locked laser via external optical feedback," IEEE J. Sel. Top. Quantum Electron. **17**(5), 1311–1317 (2011).
24. D. Arsenijević, M. Kleinert, and D. Bimberg, "Phase noise and jitter reduction by optical feedback on passively mode-locked quantum-dot lasers," Appl. Phys. Lett. **103**(23), 231101 (2013).
25. Z. G. Lu, J. R. Liu, P. J. Poole, C. Y. Song, and S. D. Chang, "Ultra-narrow linewidth quantum dot coherent comb lasers with self-injection feedback locking," Opt. Express **26**(9), 11909–11914 (2018).
26. S. Breuer, W. Elsasser, J. G. McInerney, K. Yvind, J. Pozo, E. A. J. M. Bente, M. Yousefi, A. Villafranca, N. Vogiatzis, and J. Rorison, "Investigations of repetition rate stability of a mode-locked quantum dot semiconductor laser in an auxiliary optical fiber cavity," IEEE J. Quantum Electron. **46**(2), 150–157 (2010).
27. D. Auth, S. Liu, J. Norman, J. E. Bowers, and S. Breuer, "Optical self-injection stabilization of a passively mode-locked quantum dot on silicon laser," Proc. SPIE **11301**, 113010F (2020).
28. B. Dong, X. C. de Labriolle, S. Liu, M. Dumont, H. Huang, J. Duan, J. C. Norman, J. E. Bowers, and F. Grillot, "1.3-μm passively mode-locked quantum dot lasers epitaxially grown on silicon: gain properties and optical feedback stabilization," J. Phys. Photonics **2**(4), 045006 (2020).

Optics EXPRESS

29. W. W. Chow, S. Liu, Z. Zhang, J. E. Bowers, and M. Sargent, “Multimode description of self-mode locking in a single-section quantum-dot laser,” Opt. Express **28**(4), 5317–5330 (2020).
30. T. Verolet, G. Aubin, Y. Lin, C. Browning, K. Merghem, F. Lelarge, A. Delmade, K. Mekhazni, E. Giacoumidis, and A. Shen, “Mode locked laser phase noise reduction under optical feedback for coherent DWDM communication.”,” J. Lightwave Technol. **38**(20), 5708–5715 (2020).
31. Y. Mao, J. Liu, Z. Lu, C. Song, and P. J. Poole, “Ultra-low timing jitter of quantum dash semiconductor comb lasers with self-injection feedback locking,” IEEE J. Sel. Top. Quantum Electron. **25**(6), 1–7 (2019).